

Nanocomposite Hybrid Molecular Materials for Application in Solid-State Electrochemical Supercapacitors**

By A. Karina Cuentas-Gallegos, Monica Lira-Cantú, Nieves Casañ-Pastor, and Pedro Gómez-Romero*

Molecular hybrid materials formed from polyoxometalates dispersed in conducting polymers represent an innovative concept in energy storage. This work reports in detail the first practical realization of electrodes based on these materials for energy storage in electrochemical supercapacitors. The molecular hybrids PANi/H₄SiW₁₂O₄₀, PANi/H₃PW₁₂O₄₀, and PANi/H₃PMo₁₂O₄₀ (PANi: polyaniline) have been prepared electrochemically on platinum or carbon substrates, with PANi/H₃PMo₁₂O₄₀ being the prototypical example presenting the best energy-storage performance in the series. This hybrid displays the combined activity of its organic and inorganic components to store and release charge in solid-state electrochemical capacitor cells, leading to a promising value of 120 F g⁻¹ and good cyclability beyond 1000 cycles.

1. Introduction

Energy-conversion devices such as fuel cells and renewable energy devices, such as photovoltaic or dye-sensitized solar cells, will need the support of efficient energy-storage technologies. Rechargeable lithium batteries and electrochemical supercapacitors are two of the most prominent alternatives in this respect.^[1,2] Batteries are best suited to store relatively large amounts of charge (high energy densities). However, the ion-diffusion processes are relatively slow, which is the reason why batteries score low in power-density tests, and why complementary devices related to conventional capacitors are being developed. Electrochemical supercapacitors fill in the gap between batteries and conventional capacitors, resulting in devices that provide higher power density than a battery and higher energy density than a conventional parallel-plate or double-layer capacitor.^[3,4]

Current research in electrochemical capacitors has been carried out with emphasis on the development of new electrode materials. In this line of work, we can find three kinds of electrode materials, namely, high-surface-area carbons,^[5] metal oxides,^[6–11] and conducting polymers.^[12–15] But in addition to these conventional types, novel alternative materials such as hybrid organic–inorganic nanocomposites are being considered because of their potential for synergic behavior. In this respect we mention a recent report of supercapacitor electrodes based on conducting polymers and metal oxides,^[16] and the recent

communication by our group^[17] of preliminary work on supercapacitors based on hybrid electrodes formed by conducting polymers and polyoxometalates (POMs), a work which is reported in detail in this article.

POMs resemble clusters of metal oxides, from both structural and electronic points of view; they are formed by a small number of metal centers (typically 6–18 tungsten or molybdenum moieties) coordinated by bridging oxygen atoms; they present well-known structures,^[18] and they undergo reversible multi-electron reduction processes both electrochemically and photochemically, similarly to quantum-sized oxide particles.^[19,20] Nevertheless, their solubility derived from their molecular nature, has caused them to be ignored as active compounds for electrodes or for any kind of material where collective properties were needed. POMs have been extensively studied from a chemical point of view and have been used in catalysis and photocatalysis, either as homogeneous catalyst or supported onto polymers. Some examples of POM-doped conducting organic polymers (COPs) such as polyaniline (PANi) are known; these can be applied in catalysis and in energy storage.^[21]

The similarities between POMs and oxides are not limited to their composition and topology; their electrochemical and photochemical behavior are also parallel. Thus, POMs can be electrochemically or photochemically reduced to form blue species. These reduced species are chemically and spectroscopically equivalent to tungsten or molybdenum bronzes in the form of colloidal semiconducting quantum dots, with the added advantage for POMs of a well-known structure that is stable in solution.^[20] One such structure is the Keggin structure, common to many heteropolyacids including all three studied here. In addition to their reversible redox activity, these species present high proton conductivities in their solid (acidic) form. Furthermore, they represent the ultimate limit for the dispersion of oxide species, since all metal centers can be considered to be “surface” centers, in contact with an electrolyte. All of which makes them a priori good candidates for electrode materials for electrochemical supercapacitors.

COPs, on the other hand, have been extensively studied as promising novel materials for use in rechargeable batteries^[21–25]

[*] Dr. P. Gómez-Romero, Dr. A. K. Cuentas-Gallegos, Dr. M. Lira-Cantú, Dr. N. Casañ-Pastor
Institut de Ciència de Materials de Barcelona (ICMAB)
Campus UAB
E-08193 Bellaterra (Spain)
E-mail: pedro@icmab.es

[**] This work was carried out within the framework of the “Xarxa Temàtica de Piles de Combustible de la Generalitat de Catalunya” and the “Red de Piles de Combustible del CSIC” and was partially funded by MCyT (Spain) (MAT2002-04529-C03). We also acknowledge a Ramon y Cajal contract for MLC and thank the “Consejo Nacional de Ciencia y Tecnología de México (CONACYT)” for a pre-doctoral fellowship to AKCG.

and electrochemical supercapacitors.^[26–29] Yet, one of the frequent problems related to the application of COPs is a relatively low charge-storage capacity in such devices.

The combination of conducting polymers and electroactive molecular clusters or extended inorganic species to form nanocomposite hybrid materials represents an opportunity for the design of novel materials with improved properties and enhanced energy-storage capabilities, a line of work that we have recently developed in our laboratory.^[21] In particular, the anchoring of POMs within the network of COPs such as PANi leads to the fabrication of molecular hybrid materials in which the inorganic clusters keep their integrity and activity while benefiting from the conducting properties and polymeric nature of the hybrid structure.^[21] Some of these hybrid materials have been studied in non-aqueous solvents as lithium-inserting electrodes for the potential use in lithium batteries. However, under such conditions, the electroactivity of POMs could not be harnessed for very many charge–discharge cycles.^[30] Furthermore, the electroactivity of these inorganic clusters integrated in a hybrid material is heavily dependent on the electrolyte used. Thus, the use of aqueous acidic electrolytes facilitates the counterion flux and promotes the concomitant protonation of the cluster upon reduction, leading to quick and reversible redox chemistry.^[17] All of these considerations, added to the fact mentioned above, that POM clusters offer the ultimate degree of dispersion for an oxide phase, strongly suggest that POM species could act as ideal active materials for electrochemical supercapacitors when combined with acidic electrolytes.^[31,32]

However, POMs have not been widely exploited as electrode materials for electrochemical supercapacitors. Aside from their use as electrolyte components reported in several patents^[33,34] and journals^[35] to the best of our knowledge, the use of POMs as active materials for electrochemical supercapacitors has been limited to a single report describing a device consisting of pure phosphomolybdic acid in one electrode and the widely used RuO₂ in the other.^[36]

Our preliminary communication^[17] and the full report of our work presented here are the first examples of the use of hybrid molecular nanocomposite materials formed from PANi and polyoxometalates H₄SiW₁₂O₄₀ (SiW12), H₃PW₁₂O₄₀ (PW12), and H₃PMo₁₂O₄₀ (PMo12) as electrodes in solid-state electrochemical supercapacitors.

2. Results and Discussion

2.1. PANi/SiW12

For the electrochemical synthesis of PANi/SiW12 hybrids, the scan rate was varied in order to try to deposit the greatest amount of hybrid material in a homogeneous layer. The best results were obtained for a rate of 5 mV s⁻¹ (sample SW2, 40 cycles) and consequently we repeated that experiment with more cycles (sample SW4, 60 cycles). The cyclic voltammogram of PANi/SiW12 showed a current decrease through cycling, indicating a possible conductivity loss of the working electrode.

This fact can be attributed to the deposition of SiW12 clusters on the surface of the electrode, making it less conducting.

We carried out the electrochemical characterization of these PANi/SiW12-hybrid electrodes by cyclic voltammetry (CV) in an aqueous HClO₄ solution, as described in the Experimental section. In Figure 1a we show the cyclic voltammogram corresponding to this electrochemical characterization, where we can detect the redox waves for this material. Most of them belong to PANi, except for the oxidation shoulder at -0.15 V, which can be assigned to the SiW12 polyanion.

We carried out scanning electron microscopy (SEM) investigations as part of the characterization procedure with the corresponding microanalyses, and tungsten-composition analysis for each sample. This analysis was carried out mainly to confirm whether more material was deposited when the number of cycles was increased, but using the scan rate (5 mV s⁻¹) that resulted in a more homogeneous deposit. In Figure 2 we show the corresponding SEM photos at ×300 and at ×5000 magnification, where we observe a compact deposit for sample SW2 (5 mV s⁻¹, 40 cycles), on top of which further agglomerates

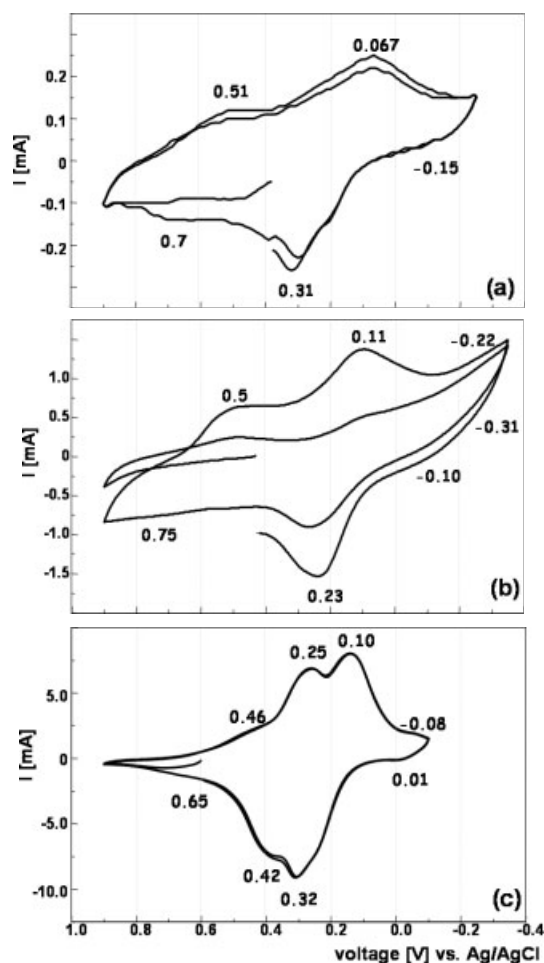


Figure 1. Characterization by CV of PANi/POM-hybrid samples carried out in a 1 M HClO₄ solution at a scan rate of 20 mV s⁻¹. The cyclic voltammograms are representative for all corresponding hybrid samples: a) PANi/SiW12, b) PANi/PW12, and c) PANi/PMo12.

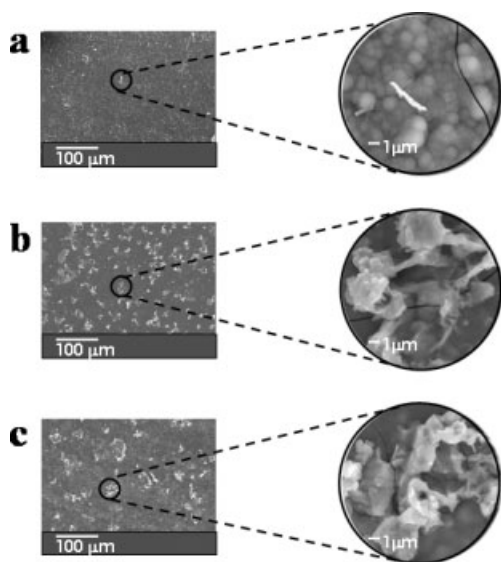


Figure 2. SEM images of PAni/SiW12 taken at a magnification of $\times 300$ (square photos) and $\times 5000$ (round photos). The materials were synthesized by CV from -0.25 to 0.9 V at a) 5 mV s^{-1} , 40 cycles (SW2); b) 2.5 mV s^{-1} , 40 cycles (SW3); and c) 5 mV s^{-1} , 60 cycles (SW4).

grow in the case of samples SW3 (2.5 mV s^{-1} , 40 cycles) and SW4 (5 mV s^{-1} , 60 cycles). As the number of cycles increased from 40 (SW2) to 60 (SW4) more material was deposited (Fig. 2c). Energy-dispersive X-ray (EDX) microanalyses of the three samples showed the presence of silicon and tungsten, confirming the presence of the SiW12 polyanion and its integration within the polymer. Finally, a mapping composition analysis confirmed a greater concentration of W in the agglomerate particles of samples SW3 and SW4.

We assembled the solid-state electrochemical supercapacitors in Swagelok cells, using two PAni/SiW12 electrodes separated by an impregnated Nafion membrane. In Table 1 we show the capacitance obtained for each hybrid sample at different current densities, cycling in a voltage range of 0–1 V. For this particular material and cells, it seems that all hybrid samples behave similarly at all current densities, resulting in very low capacitance values between 0.7 and 1.8 mF cm^{-2} . Nevertheless, as stated above, in a mapping composition analysis from SEM, we detected more tungsten from the polyanion in the agglomerate particles, making the electrode less conducting. Therefore, the supercapacitor cell assembled with electrodes made of sample SiW4 (60 cycles), which possesses a more homogeneous deposit of these agglomerate particles, resulted in lower capacitance values owing to cell resistance.

2.2. PAni/PW12

For PAni/PW12 hybrids, we carried out different experiments at different scan rates and numbers of cycles in order to deposit homogeneously the greatest amount of hybrid material. The optimal scan rate in this respect was 10 mV s^{-1} with 40 cycles (PW1D).

We carried out the electrochemical characterization of the PAni/PW12-hybrid deposit in a 1 M HClO_4 solution. Figure 1b shows the corresponding cyclic voltammogram, where we can detect and have labeled the characteristic redox waves. The couple at $0.5/0.75$ V was assigned to polyaniline, whereas the waves and shoulders around $-0.22/-0.1$ and -0.31 V were assigned to PW12, by comparison with redox waves of pure PW12. The main features at $0.11/0.23$ V could actually correspond to some overlap in the electroactivity of PAni and PW12. With the exception of sample PW1A (5 mV s^{-1} , 5 cycles, not shown here), the current increased with cycling, which indicates an increase in conductivity. This could be associated with the progressive impregnation of the hybrid electrodes with electrolyte, as successive redox cycles lead to the well-known process of swelling of PAni by impregnation with electrolyte.

We carried out an SEM investigation as part of the routine characterization procedure with the corresponding EDX microanalysis and composition analysis for each sample. In Figure 3 we show the corresponding SEM photos of all synthesized PAni/PW12 samples taken at a magnification of $\times 318$ and $\times 5000$. Looking at the photos in Figures 3a–c of samples PW1A (5 mV s^{-1} , 5 cycles), PW1C (50 mV s^{-1} , 5 cycles and 20 mV s^{-1} , 3 cycles), and PW1D (10 mV s^{-1} , 40 cycles), we can see that when using a 10 mV s^{-1} scan rate (PW1D), the particles deposited are bigger. Based on these three samples cannot be strictly compared on the basis of the electrochemical synthesis conditions, but as we mentioned above in order to obtain these hybrid materials we used different scan rates and numbers of cycles in many preliminary experiments. In sample PW1A (5 mV s^{-1} , 5 cycles) we observed a dark-blue iridescent thin layer, sample PW1C showed a dark-blue thin layer, and sample

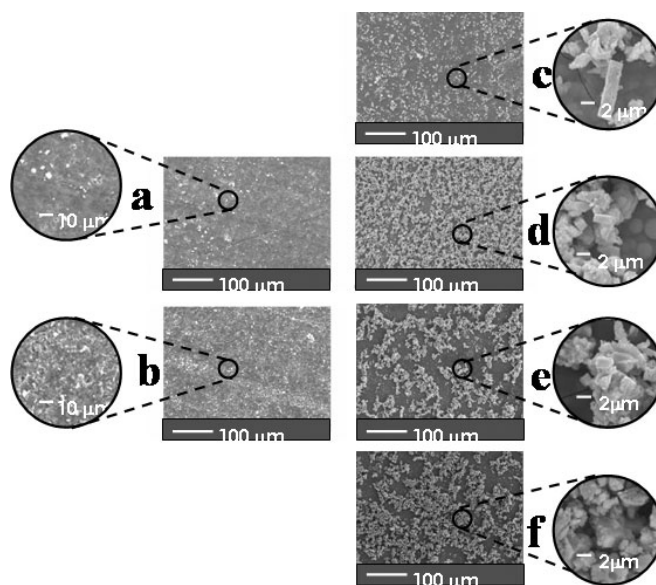


Figure 3. SEM images of samples of PAni/PW12 taken at $\times 318$ (square photos) and $\times 5000$ (round photos). The materials were synthesized by CV from 0.9 to -0.35 V at a) 5 mV s^{-1} , 5 cycles (PW1A); b) 50 mV s^{-1} , 5 cycles and 20 mV s^{-1} , 3 cycles (PW1C); c) 10 mV s^{-1} , 40 cycles (PW1D); d) 10 mV s^{-1} , 60 cycles (PW1E); e) 10 mV s^{-1} , 80 cycles (PW1F); and f) 10 mV s^{-1} , 100 cycles (PW1G).

PW1D (10 mV s⁻¹, 40 cycles) a greenish-dark-blue thin layer. Based on the SEM photographs (Figs. 3a–c) we carried out an optimization with sample PW1D (greater amount of material with bigger particles) by increasing the number of cycles.

Comparing samples PW1D (40 cycles), PW1E (60 cycles), PW1F (80 cycles), and PW1G (100 cycles) synthesized with the same scan rate (10 mV s⁻¹), we observed the formation of some yellow particles on the electrode surface, which increased in amount as the number of cycles went from 60 to 100. Only sample PW1D synthesized with 40 cycles did not present these unknown particles. In Figures 3c–f we show the SEM photographs of these samples, where sample PW1E, synthesized with 60 cycles, resulted in a layer with a larger amount of homogeneously deposited material (Fig. 3d). When we increased the number of cycles to 80 (PW1F) or 100 (PW1G), the deposit gets more heterogeneous. EDX and composition analyses (tungsten, phosphorous, and carbon) showed, in general, a homogeneous distribution of the analyzed elements; nevertheless, slight local concentrations of tungsten and phosphorous in prismatic crystals (thus from PW12) and carbon (from the polymer) were observed in the rounder particles.

We assembled symmetrical, solid-state electrochemical supercapacitor cells for PANi/PW12-hybrid samples. The hybrid samples that we used were synthesized with a 10 mV s⁻¹ scan rate, where the only difference between them was the number of cycles applied (PW1D 40 cycles, PW1E 60 cycles, PW1F 80 cycles, and PW1G 100 cycles), and the number of yellow particles on the electrode surface. In Table 1 we present the capacitance values obtained under different current densities for these PANi/PW12-hybrid samples for a voltage range of 0–1 V. Sample PW1D (40 cycles) presents the highest capacitance values for all current densities applied; these values are larger than for SiW12 cells, but still moderate. Although sam-

ple PW1E (60 cycles) had a larger amount of active material deposited homogeneously, in sample PW1D no yellow particles were observed. This fact indicates a detrimental effect of the yellow particles on the cell performance.

We tested electrodes of sample PW1D (10 mV s⁻¹, 40 cycles) in repeated charge–discharge cycles (up to 1000 cycles, Fig. 4). These data were obtained by cycling with a wider voltage window of 0–1.5 V and by applying a current density $I=1 \text{ mA cm}^{-2}$. The capacitance value decreased, starting from 6.5 mF cm⁻² to a low equilibrium value around 3 mF cm⁻². The initial capacitance value turned out to be lower than when charging the cell to a cutting voltage of 1 V, suggesting that the cutting voltage of 1.5 V is detrimental to the performance of the cell. Further experiments will need to be carried out in order to clarify the origin of this negative effect.

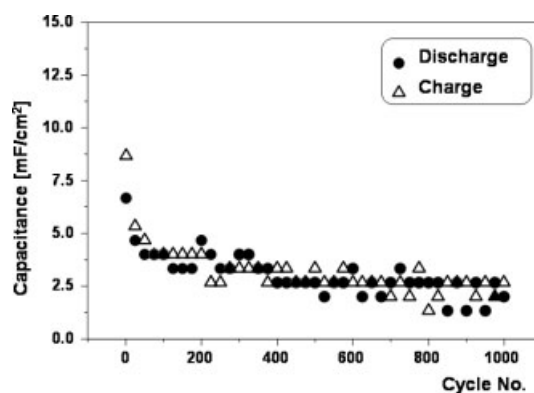


Figure 4. Charge–discharge values of a symmetrical supercapacitor, sample PW1D, in a voltage range of 0–1.5 V for 1000 cycles at $I=1 \text{ mA cm}^{-2}$.

Table 1. Capacitance values obtained by active area, for different PANi/POM-hybrid samples at different current densities.

Hybrid	Sample	Current density (I) [mA cm ⁻²]	Capacitance (C) [mF cm ⁻²]
PANi/SiW12	SiW2 (5 mV s ⁻¹ , 40 cycles)	0.5	1.65
		1	1.6
	SiW3 (2.5 mV s ⁻¹ , 40 cycles)	0.5	1.8
		1	1.2
	SiW4 (5 mV s ⁻¹ , 60 cycles)	0.5	1.3
		1	0.7
PANi/PW12	PW1D (10 mV s ⁻¹ , 40 cycles)	0.5	15
		1	13
		2	7
	PW1E (10 mV s ⁻¹ , 60 cycles)	0.5	11
		1	2
		2	1
	PW1F (10 mV s ⁻¹ , 80 cycles)	0.5	7
		1	6
		2	3
	PW1G (10 mV s ⁻¹ , 100 cycles)	0.5	5
		1	5
		2	4

2.3. PANi/PMo12

Early work on the electrochemical synthesis of PANi/PMo12 hybrids carried out by our group^[20] showed that, when using higher scan rates during the electrochemical synthesis, the deposition of the PMo12 polyanion competes with and hinders the formation of PANi. Indeed, when high scan rates for the voltage were used in synthetic CV experiments, the polyanion was first electrodeposited onto the surface of the working electrode, effectively passivating it and preventing polyaniline deposition. This is why in the present experiments hybrid electrodes were formed by first using a slower scan rate (0.5 mV s⁻¹) to deposit PANi and then a faster voltage sweep (1.5 mV s⁻¹) to increase the amount of PMo12 clusters on the surface of the electrode, increasing also the porosity, which plays an important role in electrochemical supercapacitors, as described in the Introduction.

The PANi/PMo12-hybrid electrode thus prepared was characterized via CV in 1 M HClO₄ (Fig. 1c). In this cyclic voltammogram we see two well-defined redox waves at 0.25/0.42 V and at 0.10/0.32 V characteristic of the PMo12 polyanion. Two additional redox waves corresponding to PANi can be detected as shoulders at 0.46/0.65 V and -0.08/0.01 V.

We carried out an SEM investigation and EDX microanalyses. In Figure 5 we show the corresponding SEM photos at magnifications of $\times 318$ and $\times 5000$. Microanalyses confirmed the presence of phosphorus and molybdenum throughout. Furthermore, it should be noted that the present electrodes represent a substantial improvement over those obtained in our preliminary communication^[17] in that they form a more complete and homogeneous covering of the carbon substrate by the hybrid active material.

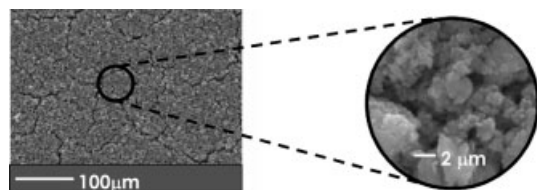


Figure 5. SEM images of a PAni/PMo12-hybrid electrode sample taken at a magnification of $\times 318$ (square photo) and $\times 5000$ (round photo).

We carried out Fourier transform infrared (FTIR) analyses of the PAni/PMo12 deposits in order to confirm the presence of PAni and the phosphomolybdate anion in the hybrid electrode. The analyses were carried out on samples obtained by carefully scraping off the material from the surface of the graphite working electrode and diluting them in KBr pellets. Figure 6 shows the FTIR spectrum of the hybrid deposit prepared as described in the Experimental section, where we can detect the characteristic bands of PAni (marked with arrows), and bands assigned to the phosphomolybdate anion (marked with circles). The peak at 1577 cm^{-1} is assigned to a deformation mode of benzene rings, the one at 1486 cm^{-1} to a deformation of benzene or quinoid rings, the ones at 1248 cm^{-1} and 1147 cm^{-1} to a C=N stretching of a secondary amine, at 1060 cm^{-1} to a P–O bond, at 955 cm^{-1} to a Mo=O terminal bond, at 876 cm^{-1} to a vertex Mo–O–Mo bond, and finally at 800 cm^{-1} to an edge Mo–O–Mo bond.

We carried out elemental analyses (% C, % H, and % N) and inductively coupled plasma (ICP) spectrometry (% Mo) of a hybrid PAni/PMo12 sample deposited onto a platinum working

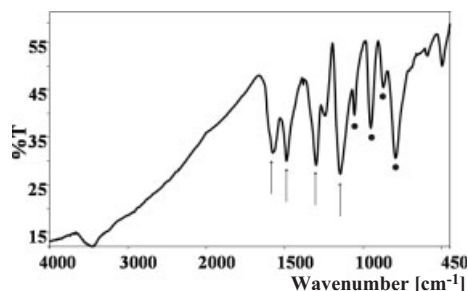


Figure 6. FTIR spectrum of a PAni/PMo12-hybrid sample (same for deposits from graphite as for Pt working electrodes), where the arrows indicate the vibrational modes of polyaniline and the circles the ones belonging to the phosphomolybdate anion.

electrode (in order to avoid any possible carbon contamination). The deposit was scraped off and the resulting powder analyzed in order to obtain the stoichiometric formula of this hybrid. The experimental values were C: 23.13 %, N: 4.30 %, H: 1.74 %, and Mo: 15.1 %. Molar ratios are close to the expected values (C/N ratio 6.2, C/Mo ratio 12.2 (i.e., 24.5 C6 per PMo12), H/N ratio 5.66) and indicate a material of formula $\text{C}_6\text{H}_5\text{N}(\text{PMo}_{12}\text{O}_{40})_{0.042}\cdot\text{H}_2\text{O}$ (formula weight, FW = 185.6). However, the percentage values calculated for this formula (C 38.8, N 7.54, H 3.8, Mo 26.0) are all higher than the experimental ones. This indicates the presence of some undetected impurity (not containing C, N, H, or Mo), most likely metallic platinum scraped off the electrode. Aside from this impurity, all the experimental molar ratios between C, H, Mo, and N confirm the formula of a material containing approximately 24 aniline rings per PMo12 unit.

We carried out different analyses in solid-state electrochemical supercapacitor cells, set up as described in the Experimental section, based on PAni/PMo12 electrodes. In Figure 7a we show how the capacitance (normalized per effective electrode area) of our symmetrical cell varies as a function of applied current density, cycling between 0 and 1 V. As expected, the discharge capacitance values are larger at slow current densities. However, it should be noted that the decrease in capaci-

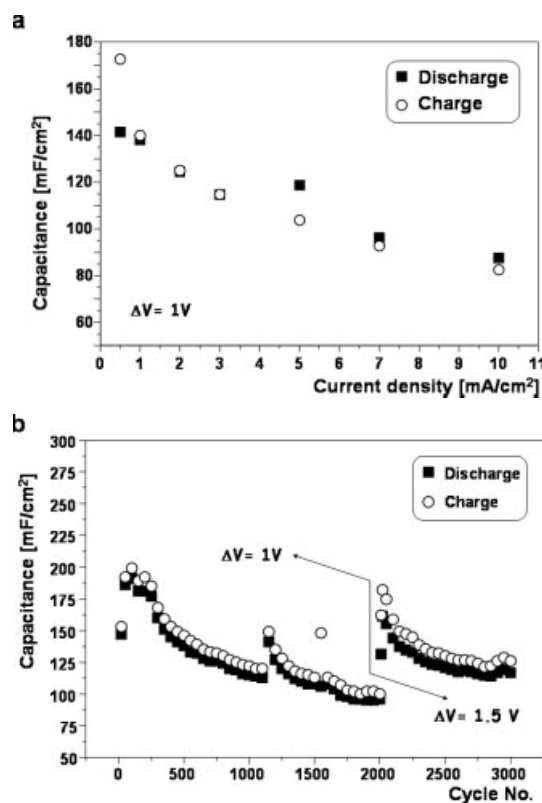


Figure 7. Electrochemical supercapacitor behavior of a PAni/PMo12 hybrid (normalized with respect to the electroactive area). a) Capacitance values per square area at different current densities using a voltage window of $\Delta V = 1\text{ V}$; and b) successive charge–discharge cycles at $I = 1\text{ mA cm}^{-2}$, where the first 2000 cycles are carried out with a voltage window of $\Delta V = 1\text{ V}$ and the following 1000 cycles with a voltage window of $\Delta V = 1.5\text{ V}$.

tance with increasing current density is relatively small, amounting to a 35 % decrease (from 140 to 90 mF cm⁻²) for a one order of magnitude increase in current density (from 1 to 10 mA cm⁻²).

In Figure 7b, we show the evolution of capacitance in successive charge–discharge cycles using a 1 mA cm⁻² current density. The first 2000 cycles were carried out between 0 V and 1 V, and the following 1000 cycles between 0 V and 1.5 V. During the first 2000 cycles, we observe that the capacitance declines from a starting value of 200 mF cm⁻² to a value of around 110 mF cm⁻². We note two instances in which the continuity of the cycling activity is accidentally disturbed, and the system was able to relax (around cycles 1200 and 1600). In the following 1000 cycles, another jump in the capacitance to higher values (up to 165 mF cm⁻²) was induced by a controlled change in the cycling regime involving an increase in the voltage range ($\Delta V = 1.5$ V). The capacitance then decreases and stabilizes at values around 120 mF cm⁻² (30 % loss in 1000 cycles)—remarkably, a better stabilization and at a slightly higher capacitance than that reached after the first 1000 cycles under the one-volt regime. These recoveries of cell capacitance point out the importance of cell design and routine-discharge features in addition to the intrinsic energy-storage properties of the materials themselves, and they remind us of the need to keep working on factors related to cell optimization and the possibilities to improve performance through the engineering of these systems.

Up to this point, we have discussed performance based on capacitance values normalized per effective surface area of our electrodes [mF cm⁻²]. However, from a technological point of view, materials science studies in this field rely upon measurements in terms of farads per gram, that is, with the capacitance normalized per unit mass of active material. In order to calculate the capacitance per active mass, we carried out successive electrochemical syntheses of a PAni/PMo12-hybrid sample onto a platinum-foil working electrode. After each synthesis, the material was collected by scraping it off the working electrode. The greenish solid obtained was washed with deionized water until all blue color disappeared (elimination of excess phosphomolybdic acid), and was dried under vacuum for three days. This hybrid material presented the same FTIR spectrum as the hybrid deposited onto graphite, and its formula is discussed above. After weighing the active hybrid material, we proceeded to fabricate a film following the procedure described in the Experimental section.

In Figure 8a we show the capacitance per active mass obtained at different current densities, always cycled between 0 and 1 V. Again, at lower current densities the capacitance is higher, but with a larger mismatch between measured charge and discharge capacitances. It should be noted that Figure 8a includes two extra points at $I = 125$ mA cm⁻² (a charge and a discharge value), which belong to an average of four cycles, determined after collecting the data for each current density applied. These extra points were measured to confirm the reproducibility of the values obtained. Figure 8a also presents the data measured with cells fabricated with electrodes containing only PMo12 as the active component (i.e., without PAni) in film electrodes prepared as above. In addition, we have in-

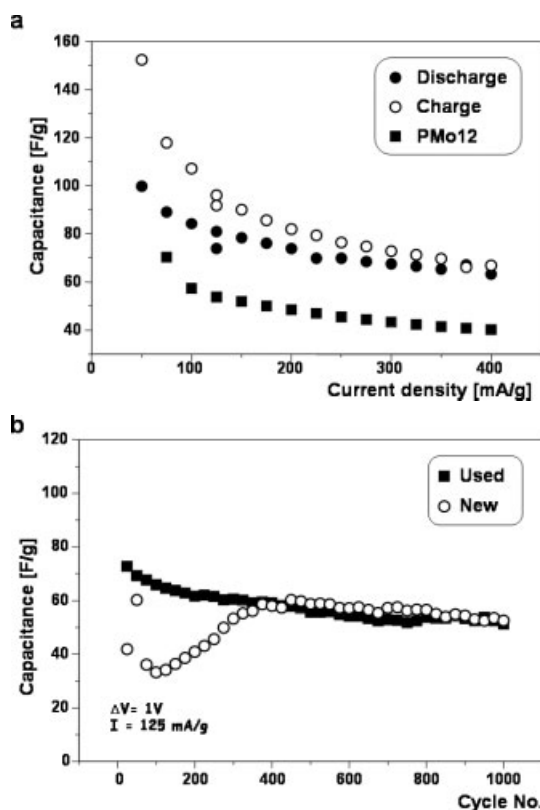


Figure 8. Electrochemical supercapacitor behavior of a PAni/PMo12 hybrid (normalized with respect to the active mass). a) Capacitance values at different current densities at $\Delta V = 1$ V (for comparison, PMo12-polyanion film electrodes without polyaniline are shown); b) successive charge–discharge cycles of new and used electrodes at $I = 125$ mA g⁻¹ carried out with a voltage window of $\Delta V = 1$ V.

cluded the performance of a symmetrical cell based on just the polyoxometalate for comparison. Indeed, the capacitances obtained for the PMo12 cell was smaller than those from cells making use of the hybrid material, confirming the combined effect of both the organic polymer and the inorganic cluster in the performance of the PAni/PMo12-hybrid electrodes.

In addition to the intrinsic properties of our materials, we have also detected and studied the effect of additional factors related to kinetics, cell design, and “history” of the electrodes. For instance, in Figure 8b we compare the successive charge–discharge cycles of two supercapacitor devices using new and used electrodes (same capacitor as shown in Fig. 8a), applying a current density of 125 mA g⁻¹. We can observe how the capacitance values stabilize for both cells at similar values of 50–60 F g⁻¹. However, the initial behavior of each of the cells is quite different. For the device assembled with used electrodes, we get a higher initial capacitance value of 75 F g⁻¹. On the other hand, when using new electrodes, the supercapacitor performance seems to reach a maximum after a few cycles; that is, an electrochemical activation of the electrodes seems to be required, which is achieved through repeated cycling. The starting value of the capacitance for the new electrodes was 40 F g⁻¹ (lower than of the used electrodes), increasing during the first

300 cycles through an apparent electroactivation process to eventually reach the same stabilized value mentioned above.

The fact that this electroactivation process takes place only for self-standing composite films and not for the electrochemically prepared deposits indicates a kinetic origin of the phenomenon, probably more related to the microstructural engineering of the films than to intrinsic material properties. In particular, it could be related to the need to open up the structure of the polymer in the self-standing samples for proper electrolyte impregnation at a molecular level, in agreement with the well-known swelling and solvent impregnation of conducting polymers during electrochemical cycling.^[37]

We carried out experiments increasing the voltage window up to 1.5 V, as we had done for electrochemical deposits, but in this case during recharge we could not reach the cutting voltage of 1.5 V. Thus, our final experiments with an increased voltage range were limited to a 1.2 V polarization. In Figure 9a we show the capacitance values obtained at different current densities. Surprisingly, the capacitance values increase with increasing current densities. This could be assigned to the increase of the voltage window, or to the electroactivation process, but will need more studies to confirm its cause. However, the higher mismatches of the charge and discharge capacitance values are also observed for lower intensities. In Figure 9b we show the variation in capacitance with successive charge–discharge cycles using a current density of 400 mA g⁻¹ (best matching of charge and discharge capacitance values) in the device shown in Figure 9a (used electrodes). We observe an increase of the capacitance value from 65 F g⁻¹ to 110–120 F g⁻¹. In addition, during the first 300 cycles the capacitance value increases gradually, indicating an electroactivation process of the electrodes under the given conditions ($\Delta V = 1.2$ V, $I = 400$ mA g⁻¹). Finally, we can observe no mismatch between the charge and discharge values, indicating excellent reversibility of the overall polarization process. In Figure 9c we show the charge–discharge profiles measured at 400 mA g⁻¹ for the device shown in Figure 9a.

We carried out more electrochemical studies with new electrodes (not electroactivated) under different current densities cycling between 0 and 1 V in order to try to understand the factors that influence the electroactivation process described above. In Figure 10 we show the results of this study. First, we used a high current density of $I = 400$ mA g⁻¹ for the first 2000 cycles and obtained very low capacitance values between 3 and 10 F g⁻¹. Then a lower current density of $I = 125$ mA g⁻¹ was applied for 300 cycles, to activate the electrode (conditions extracted from the experiments shown in Fig. 8b), resulting in a rapid increase of the capacitance up to 100 F g⁻¹, which marks the electroactivation process. Finally, we carried out 2000 cycles more, again at a higher current density of $I = 400$ mA g⁻¹. We observed a decrease of the capacitance down to 60 F g⁻¹ in the first cycle, then a continuous increase followed by a jump in cycle 3300 (cycle 1000 of the 2000 with $I = 400$ mA g⁻¹)—an improvement from 75 F g⁻¹ to 110 F g⁻¹. This value of 110 F g⁻¹ decreased slowly to 75 F g⁻¹ at the end of the experiment, after more than 4000 cycles. Furthermore, we carried out experiments with a symmetrical supercapacitor cell with PMo12 in a

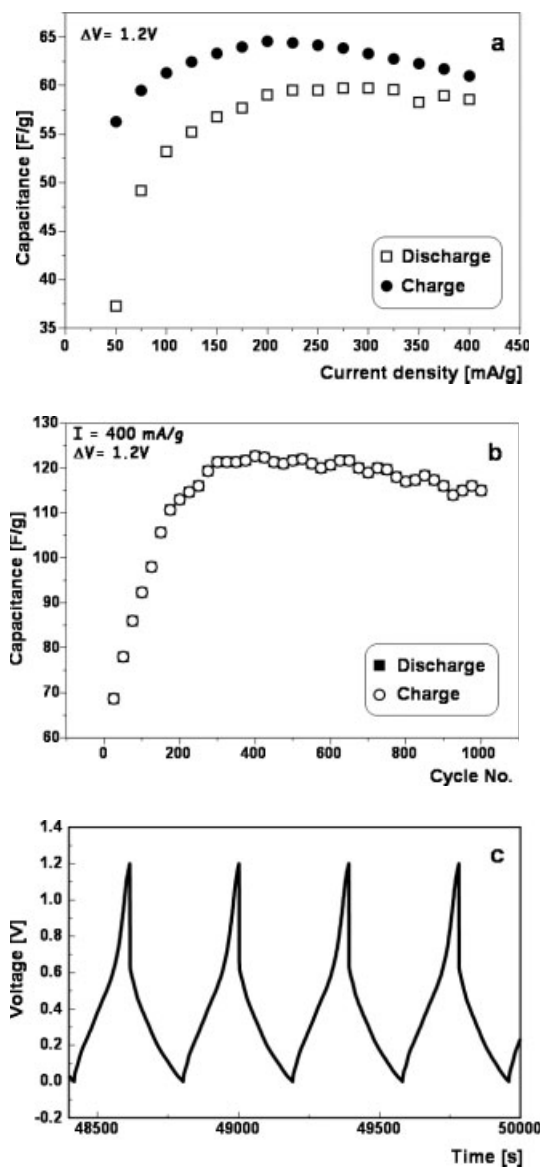


Figure 9. Electrochemical supercapacitor behavior of PANi/PMo12. Capacitances are normalized per mass of active material. a) Capacitance versus current density with $\Delta V = 1.2$ V; b) evolution of capacitance with successive charge–discharge cycles at $I = 400$ mA g⁻¹ for the same cell ($\Delta V = 1.2$ V); and c) first four cycles measured at 400 mA g⁻¹ (same cell used for the datum at 400 mA g⁻¹ in Figure 9a, i.e., after 60 cycles under varying current densities).

composite film electrode (i.e., instead of the PANi/PMo12 hybrid) and show the results in the same figure to determine if an electroactivation process could also be detected for the purely inorganic active material. The analysis was carried out by applying a fast charge–discharge rate ($I = 400$ mA g⁻¹) for the first 1000 cycles, and then, in the following 300 cycles, the same lower current density ($I = 125$ mA g⁻¹) to allow for a possible electroactivation process. During the first 1000 cycles we observed a decrease in capacitance from 38 F g⁻¹ to 6.4 F g⁻¹. In the following 300 cycles the capacitance continued to decrease to a value of 1.9 F g⁻¹; thus no electroactivation process was de-

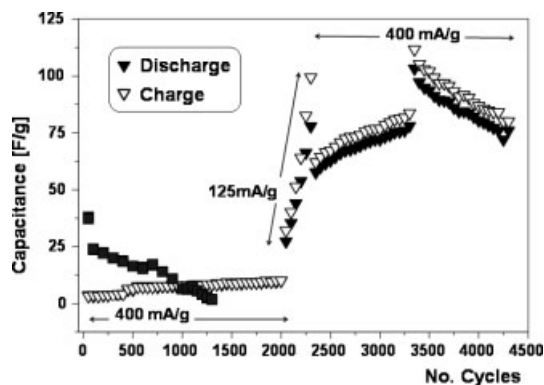


Figure 10. Electrochemical studies of supercapacitors with new electrodes in the voltage range 0 to 1 V. For the PANi/PMo12 hybrid, the applied current density for the first 2000 cycles was 400 mA g^{-1} , 125 mA g^{-1} for the next 300 cycles, and finally 400 mA g^{-1} for the next 2000 cycles. For comparison, the performance of electrodes based on PMo12 (■) is shown. In the first 1000 cycles we applied a current density of 400 mA g^{-1} ; the next 300 cycles were measured at 125 mA g^{-1} .

tected for the electrodes containing only the inorganic components (otherwise fabricated identically to the hybrid-containing electrodes); in this case the capacity to store charge was decreased. These results confirm the conducting polymer to be at the origin of the electroactivation process, a process which needs slow current densities and is independent of the voltages used in our experiments. This is in agreement with the electrolyte impregnation through swelling that takes place in this type of material upon cycling and which was mentioned above.

3. Conclusions

We have carried out the synthesis and have successfully fabricated composite bulk electrodes of molecular hybrid materials based on polyaniline (PANi) and polyoxometalates (POMs) for possible application in electrochemical supercapacitor devices. Thus, we have successfully prepared, by electrochemical methods, deposits of the hybrid PANi/PMo12 on graphite and have used this material to set up symmetrical cells with H_2SO_4 -impregnated Nafion as the electrolyte. These cells can be repeatedly cycled for thousands of cycles (at least 4000) with only a small loss of capacity. Values of 120 F g^{-1} can be reached, which compare very favorably with the more modest values of $70\text{--}40 \text{ F g}^{-1}$ for the purely inorganic active material (furthermore, cyclability is much better for the hybrid). These results point out a very encouraging preliminary performance and open the door for a possible application of this type of hybrid material in electrochemical supercapacitors. We have detected a characteristic behavior concerning the activity of these molecular hybrids, which need an electroactivation process in order to reach their optimal performance. This electroactivation process in the hybrid is due to kinetic aspects not attributed to the inorganic component of the molecular hybrid material, but most likely related to the characteristic swelling of conducting organic polymers^[37] (as has been previously detected in other

molecular hybrids), resulting in a progressive impregnation with electrolyte during the first cycles. In the electrochemical deposits, this electroactivation seems to be easier (Fig. 7b), as expected for a thinner film deposit, which has a larger interface with the electrolyte.

We have also prepared electrodes with PANi/SiW12 and PANi/PW12 as active materials; however, the cells based on these electrodes led to poorer preliminary results than those based on PANi/PMo12, both with respect to capacities ($1\text{--}14 \text{ mF cm}^{-2}$) and number of cycles.

The molecular hybrid materials described in this paper, and very particularly the PANi/PMo12, in which the electroactivity of both components is well-matched, constitute very promising, novel systems for energy storage as electrochemical supercapacitors.

4. Experimental

Phosphomolybdic acid ($\text{H}_3\text{PMo}_{12}\text{O}_{40} \cdot n\text{H}_2\text{O}$ FW = 1825.24, PMo12), silicotungstic acid 99.9% ($\text{H}_4\text{SiW}_{12}\text{O}_{40} \cdot n\text{H}_2\text{O}$ FW = 2878.29, SiW12), and phosphotungstic acid ($\text{H}_3\text{PW}_{12}\text{O}_{40} \cdot n\text{H}_2\text{O}$ FW = 2880.17, PW12) were purchased from Aldrich and used as received. Aniline was obtained from Fluka (distilled under reduced pressure before use), and HCl from Panreac was used as received.

All electrodes used for the electrochemical synthesis of PANi/POMs, were purchased from Goodfellow: a rigid graphite plate (99.95%, 0.25 mm thick, 1.3 cm \times 5 cm), and Pt foil (0.01 mm thick, 1.5 cm \times 5 cm).

To fabricate the film electrodes to be used in supercapacitor cells, we used Kinar-flex (binder agent, also known as PVDF (poly(vinylidene fluoride))) provided by Elfatochem, super-P, which is amorphous carbon (Brunauer–Emmett–Teller (BET) surface area of $60 \text{ m}^2 \text{ g}^{-1}$) provided by MMM Belgium, acetone purchased from Panreac, and finally, dibutyl phthalate (DBP) provided by Aldrich.

Electrochemical measurements were carried out in a PAR273A potentiostat (Princeton, USA). A standard three-electrode cell was used for the preparation of film deposits, composite films, and for electrochemical measurements. The reference electrode used was Ag/AgCl (0.197 V vs. NHE (normal hydrogen electrode)). The working electrodes to prepare active materials for electrochemical supercapacitors were prepared electrochemically, both as thin-film deposits and as thicker deposits for bulk (mass) characterization. In the first case, the working electrode used was a rigid graphite plate (0.025 mm thick, 1.3 cm \times 5 cm), where one of the sides was covered with an insulating plastic tape and only a surface of 1.3 cm \times 2.5 cm was exposed. For bulk syntheses a Pt sheet (0.01 mm thick, 1.5 cm \times 5 cm) was used as working electrode and the materials deposited were scraped off. The counter electrode used for the experiments dealing with thin-film deposits consisted of Pt foil (0.01 mm thick, 1.5 cm \times 5 cm), whereas for the synthesis of bulk materials a Pt coil was used.

Surface and microstructure analyses of the hybrid deposits were carried out using a Hitachi S-570 SEM, with EDX and composition analyses in some cases. FTIR analyses were carried out in a Nicolet 710 FTIR spectrophotometer in dilute KBr pellets made of the scraped-off samples. Elemental analyses were carried out in a Carlo Erba CHN EA 1108 at a maximum combustion temperature of 1800°C , and ICP analysis was performed using a Thermo Jarrell-Ash model 61E Polyscan multichannel apparatus under standard conditions.

Electrochemical supercapacitor cells were tested in a multichannel charge–discharge galvanostatic analyzer (Arbin Instruments, College Station, USA).

The hybrid electrodes of the different materials were prepared as thin-film deposits on the graphite foil using a CV technique at room temperature. First, PANi/SiW12 hybrids were electrochemically synthesized using a suspension made by mixing 5.23 g of silicotungstic acid with 1 mL of aniline and adding 100 mL of water, in a voltage range of

0.9 to -0.25 V versus Ag/AgCl using different scan rates (2.5, 5, or 10 mV s^{-1}) and different numbers of cycles to obtain four different samples. Then, PANi/PW12 hybrids were electrochemically synthesized using a suspension made by mixing 7.89 g of phosphotungstic acid with 1 mL of aniline and adding 100 mL of water, in a voltage range of 9 to -0.35 V versus Ag/AgCl using different scan rates and number of cycles, leading to six different samples. Finally, PANi/PMo12 hybrids, in both cases (thin-film deposits and thicker deposits for bulk experiments), were synthesized from a suspension made by mixing 5 g of phosphomolybdic acid with 1 mL of aniline and then adding 100 mL of water, in a voltage range of 9 to -0.1 V versus Ag/AgCl and two different scan rates (0.5 mV s^{-1} and 1.5 mV s^{-1}) to yield only one sample. All suspensions were prepared using deionized water.

After the PANi/POM syntheses, the coated graphite electrodes were electrochemically characterized using the same three-electrode cell setup (Pt plate was used as counter electrode and Ag/AgCl as the reference) in a 1 M $\text{HClO}_4(\text{aq})$ electrolyte solution, the same electrochemical technique (CV) and with a scan rate of 20 mV s^{-1} .

Electrochemical supercapacitor cells were assembled as symmetrical devices (i.e., with two identical electrodes) in a typical Swagelok cell [38]. Three voltage ranges were used: 0 to 1 V, 0 to 1.2 V, and 0 to 1.5 V, depending on the experiment. The hybrid thin-film deposits on graphite were cut into 6 mm \times 6 mm electrodes, for their direct use in the supercapacitor-cell assembly. For quantitative analyses of bulk samples (capacitance to be normalized per unit of mass in supercapacitor cells), the hybrid materials deposited on the Pt-plate electrode was scraped off and used to prepare a composite microporous film as follows. A suspension of 52 wt.-% of the active hybrid material, 22 wt.-% of Kinar flex as binder, and 24 wt.-% of carbon super-P, and three drops of DBP in 2 mL of acetone were thoroughly mixed and stirred for 12 h to yield a homogeneous paste. The paste was tape-cast onto a glass surface and the acetone allowed to evaporate. After peeling off the resulting film it was washed with diethyl ether in order to remove DBP. This process allows the formation of a porous microstructure in the film. Discs 1 cm in diameter were cut to assemble the cell. The active hybrid material used for the fabrication of films was washed with deionized water until no color was seen in the residual water, and dried under vacuum for three days.

In the supercapacitor devices, a solid-electrolyte membrane of commercial Nafion 117 (perfluorinated membrane, 12 mm-diameter discs, 0.1778 mm thick) was used as separator and electrolyte after impregnation with sulfuric acid following a standard procedure [39]. In cells where different current densities were tested, the capacitance value for each current density was calculated as an average of four successive charge-discharge cycles. In all experiments the specific capacitance value was calculated based on the active mass or active area of a single electrode.

Received: July 20, 2004

- [1] J. H. Edwards, S. P. S. Badwal, G. J. Duffy, J. Lasich, G. Ganakas, *Solid State Ionics* **2002**, 152–153, 843.
- [2] R. M. Dell, D. A. J. Rand, *J. Power Sources* **2001**, 100, 2.
- [3] R. Kötz, M. Carlen, *Electrochim. Acta* **2000**, 45, 2483.
- [4] B. E. Conway, *Electrochemical Supercapacitors. Scientific Fundamentals and Technological Applications*, Kluwer Academia/Plenum Publishers, New York **1999**.

- [5] J. P. Zheng, J. Huang, T. R. Jow, *J. Electrochem. Soc.* **1997**, 144, 2026.
- [6] T. Kudo, Y. Ikeda, T. Watanabe, M. Hibino, M. Miyayama, H. Abe, K. Kajita, *Solid State Ionics* **2002**, 152–153, 833.
- [7] J. Jiang, A. Kucernak, *Electrochim. Acta* **2002**, 47, 2381.
- [8] M. Wohlfahrt-Mehrens, J. Schenk, P. M. Wilde, E. Abdelmula, P. Axmann, J. Garche, *J. Power Sources* **2002**, 105, 182.
- [9] C. C. Hu, T. W. Tsou, *J. Power Sources* **2003**, 115, 179.
- [10] H. Kim, B. N. Popov, *J. Electrochem. Soc.* **2003**, 150, D56.
- [11] N. L. Wu, S. Y. Wang, C. Y. Han, D. S. Wu, L. R. Shiue, *J. Power Sources* **2003**, 113, 173.
- [12] M. Mastragostino, C. Arbizzani, F. Soavi, *Solid State Ionics* **2002**, 148, 493.
- [13] J. H. Park, O. O. Park, *J. Power Sources* **2002**, 111, 185.
- [14] K. S. Ryu, K. M. Kim, N. G. Park, Y. J. Park, S. H. Chang, *J. Power Sources* **2002**, 103, 305.
- [15] W. C. Chen, T. C. Wen, T. Hsisheng, *Electrochim. Acta* **2003**, 48, 641.
- [16] S. A. Hashmi, H. M. Upadhyaya, *Ionics* **2002**, 8, 272.
- [17] P. Gómez-Romero, M. Chojak, A. K. Cuentas-Gallegos, J. A. Asensio, P. J. Kulesza, N. Casañ-Pastor, M. Lira-Cantú, *Electrochem. Commun.* **2003**, 5, 149.
- [18] M. T. Pope, A. Müller, in *Polyoxometalates: From Platonic Solids to Antiretroviral Activity*, Topics in Molecular Organization and Engineering, Kluwer, Dordrecht, The Netherlands **1994**.
- [19] P. Gómez-Romero, N. Casañ-Pastor, *J. Phys. Chem.* **1996**, 100, 12448.
- [20] P. Gómez-Romero, *Solid State Ionics* **1997**, 101–103, 243.
- [21] P. Gomez-Romero, *Adv. Mater.* **2001**, 13, 163.
- [22] B. Scrosati, *Prog. Solid State Chem.* **1988**, 18, 1.
- [23] C. Barbero, M. C. Miras, B. Schryder, O. Haas, R. Kötz, *J. Mater. Chem.* **1994**, 4, 1775.
- [24] N. Oyama, T. Tatsuma, T. Sato, T. Sotomura, *Nature* **1995**, 373, 598.
- [25] P. Novak, K. Muller, K. S. V. Santhanam, O. Haas, *Chem. Rev.* **1997**, 97, 207.
- [26] K. R. Prasad, N. Munichandraiah, *J. Power Sources* **2002**, 112, 443.
- [27] K. S. Ryu, K. M. Kim, Y. J. Park, N. G. Park, M. G. Kang, S. H. Chang, *Solid State Ionics* **2002**, 152–153, 861.
- [28] S. A. Hashmi, H. M. Upadhyaya, *Solid State Ionics* **2002**, 152–153, 883.
- [29] W. C. Chen, T. C. Wen, *J. Power Sources* **2003**, 117, 273.
- [30] P. Gómez-Romero, M. Lira-Cantú, *Adv. Mater.* **1997**, 9, 144.
- [31] G. Torres-Gómez, M. Lira-Cantú, P. Gómez-Romero, *J. New Mater. Electrochem. Syst.* **1999**, 2, 145.
- [32] P. J. Kulesza, M. A. Malik, B. Karwowska, K. Miecznikowski, W. Dzwolak, A. Wolkiewicz, A. Gursynska, I. N. Grzybowa, *Electrochemical Capacitors, Proc.* (Eds: F. M. Delnick, D. Ingersoll, X. Andrieu, K. Naoi) Electrochemical Society, Pennington, UK **1997**, PV 96-2, p. 89.
- [33] C. Li, R. H. Reuss, M. Chason, *US Patent 5 847 920*, **1999**.
- [34] C. Li, R. H. Reuss, *US Patent 5 986 878 A*, **1999**.
- [35] G. Alberti, M. Casciola, *Annu. Rev. Mater. Res.* **2003**, 33, 129.
- [36] A. Yamada, J. B. Goodenough, *J. Electrochem. Soc.* **1998**, 145, 737.
- [37] G. Torres-Gómez, *Ph.D. Thesis*, Universitat Autònoma de Barcelona, **2001**.
- [38] D. Guyomard, J. M. Tarascon, *J. Electrochem. Soc.* **1991**, 139, 937.
- [39] R. Savinell, E. Yeager, D. Tryk, U. Landau, J. Wainright, D. Weng, K. Lux, M. Litt, C. Rogers, *J. Electrochem. Soc.* **1994**, 141, L46.